Biosynthesis of poly(glycolate-*co*-3-hydroxybutyrate-*co*-3-hydroxyhexanoate) in *Escherichia coli* expressing sequence-regulating polyhydroxyalkanoate synthase and medium-chain-length 3-hydroxyalkanoic acid coenzyme A ligase

Hiroya Tomita,[1] Keigo Satoh,[2] Christopher T. Nomura,[3] and Ken'ichiro Matsumoto[1]*

[1]Division of Applied Chemistry, Faculty of Engineering, Hokkaido University, N13W8, Kitaku, Sapporo 060-8628, Japan

[2]Graduate School of Chemical Sciences and Engineering, Hokkaido University, N13W8, Kitaku, Sapporo 060-8628, Japan

[3]Department of Biological Sciences, University of Idaho, 875 Perimeter Drive, Moscow, ID, 83844, USA

*To whom correspondence should be addressed:

Prof. Ken'ichiro Matsumoto, Division of Applied Chemistry, Faculty of Engineering, Hokkaido University, N13W8, Kitaku, Sapporo 060-8628, Japan, Telephone: (+81)-11-706-6610, E-mail: mken@eng.hokudai.ac.jp

Running title: A glycolate-based polyhydroxyalkanoate terpolymer

Keywords: polyhydroxyalkanoate, block copolymer, glycolate, 3-hydroxyhexanoate

Abstract

Chimeric polyhydroxyalkanoate synthase $PhaC_{AR}$ is characterized by the capacity to incorporate unusual glycolate (GL) units and spontaneously synthesize block copolymers. The GL and 3-hydroxybutyrate (3HB) copolymer synthesized by $PhaC_{AR}$ is a random-homo block copolymer, poly(GL-*ran*-3HB)-*b*-poly(3HB). In the present study, medium-chain-length 3-hydroxyhexanoate (3HHx) units were incorporated into this copolymer using $PhaC_{AR}$ for the first time. The coenzyme A (CoA) ligase from *Pseudomonas oleovorans* (AlkK) serves as a simple 3HHx-CoA supplying route in *Escherichia coli* from exogenously supplemented 3HHx. NMR analyses of the obtained polymers revealed that 3HHx units were randomly connected to 3HB units, whereas GL units were heterogeneously distributed. Therefore, the polymer is composed of two segments: P(3HB-*co*-3HHx) and P(GL-*co*-3HB-*co*-3HHx). The thermal and mechanical properties of the terpolymer indicate no contiguous P(3HB) segments in the material, consistent with the NMR results. Therefore, $PhaC_{AR}$ synthesized the novel block copolymer P(3HB-*co*-3HHx)-*b*-P(GL-*co*-3HB-*co*-3HHx), which is the first block PHA copolymer comprising two copolymer segments.

Polyhydroxyalkanoates (PHAs) are bacterial storage polyesters that can be produced from various renewable biomass and used as plastic materials (Zhang *et al.* 2018; Bedade *et al.* 2021). PHA synthase (PhaC) plays a central role in the biosynthetic pathway of PHAs (Rehm 2003). PhaC is typically specific to 3-hydroxyacyl-coenzyme A (CoA) substrates (Steinbüchel and Hein 2001; Sudesh et al. 2000) and synthesizes homopolymers and/or random copolymers, which have no regulated monomer sequence, with multiple monomer substrates (Doi et al. 1995; Bartels *et al.* 2020).

Sequence-regulating PhaC is a recently discovered type of enzyme which is

capable of spontaneously synthesizing block copolymers without the manipulation of feedstocks during cultivation (Matsumoto *et al.* 2018). $PhaC_{AR}$, which is a unique sequence-regulating PHA synthase, is an engineered chimeric enzyme composed of PHA synthases from *Aeromonas caviae* and *Ralstonia eutropha* (*Cupriavidus necator*) (Matsumoto *et al.* 2009). Notably, $PhaC_{AR}$ possesses unusual substrate specificity toward glycolyl (GL)-CoA (Arai *et al.* 2020). We previously reported that $PhaC_{AR}$ synthesized a block copolymer of GL and 3-hydroxybutyrate (3HB), poly(GL-*ran*-3HB)-*b*-poly(3HB).

GL-based polymers are characterized by their high hydrolytic degradability. For example, chemically synthesized polyglycolic acid (PGA) and poly(lactide-*co*-glycolide) (PLGA) can be hydrolyzed without the action of esterases (Pandita, Kumar and Lather 2015). Such hydrolytically degradable polymers have the potential to undergo hydrolysis in animal tissues; thus, they have the potential to serve as rapidly bioabsorbable materials (Pervaiz *et al.* 2019; Shawe *et al.* 2006). In contrast, natural PHAs have low hydrolytic degradability and slow bioabsorption (Basnett *et al.* 2018; Chen and Zhang 2018). GL-based PHAs potentially exhibit an intermediate hydrolytic degradability between chemically prepared GL-based polymers and natural PHAs. In fact, the first GL-based PHA random copolymer P(GL-*co*-3HB) synthesized using $PhaC1_{Ps}$STQK hydrolyzes in the absence of PHA depolymerases (Matsumoto *et al.* 2011; Matsumoto *et al.* 2017).

P(GL-*ran*-3HB)-*b*-P(3HB) synthesized by $PhaC_{AR}$ contains 23 mol% GL, which is higher than that of $PhaC1_{Ps}$STQK (16 mol%) obtained under the same culture conditions (Arai 2020). The block copolymer contains a GL-rich segment with a local GL fraction of 71 mol%, indicating the superior GL-incorporating capacity of $PhaC_{AR}$. However, a drawback of P(GL-*ran*-3HB)-*b*-P(3HB) is the stiff and brittle properties of the produced material. A potentially effective strategy to improve the material properties of PHA is the incorporation of 3-hydroxyhexanoate (3HHx) units into the polymer. A successful example is P(3HB-*co*-3HHx), also known as PHBH (Sato *et al.* 2015), which

exhibits higher flexibility than P(3HB) (Wong *et al.* 2012). Here, we report the incorporation of 3HHx as the third monomer into the copolymer with GL and 3HB repeating units by $PhaC_{AR}$ to improve the physical properties. Analysis of the structure and physical properties of the obtained polymer indicated that they are representative of a new GL-based block terpolymer with transparent and superior extensible properties.

To supply 3HHx-CoA, 3-hydroxyacyl-CoA ligase from *Pseudomonas oleovorans* (AlkK) (Wang *et al.* 2012) was utilized. In PHA-producing *Pseudomonas* strains, the enzyme serves as a *de novo* medium-chain-length (MCL) monomer-supplying pathway together with the 3-hydroxyacyl-acyl carrier protein thioesterase (PhaG) (Rehm, Krüger and Steinbüchel 1998; Wang 2012). The *alkK* gene is functionally expressed in *Escherichia coli* (Satoh *et al.* 2005). Heterologous expression of PhaG and AlkK in *E. coli* enables the synthesis of MCL PHA from non-fatty acid carbon sources (Scheel *et al.* 2019; Tappel *et al*. 2014). In the present study, we utilized AlkK to supply 3HHx-CoA from exogenous 3HHx supplemented into the medium. This enzyme serves as an easy-to-use 3HHx-CoA supplying route in *E. coli*.

Materials and Methods

Plasmid construction for polymer production.

A plasmid for synthesizing P(GL-*co*-3HB-*co*-3HHx) was constructed based on $pBSP_{Re}phaC_{AR}pct$ (Matsumoto *et al.* 2018). An *Afl*II recognition site was introduced downstream of the *pct* gene. Using this site, *alkK* from *P. oleovorans*, which encodes acyl-CoA ligase, was introduced. The resulting plasmid $pBSP_{Re}phaC_{AR}pctalkK$ was confirmed not to possess any unintended mutations.

Preparation of 3HHx

Ethyl (*R,S*)-3-hydroxyhexanoate was hydrolyzed by adding an excess amount of 10 N NaOH on ice until the solution was no longer phase separated. The solution was acidified to approximately pH 2 by adding 6 N HCl, and diethylether was then added to extract 3-hydroxyhexanoic acid. Diethylether was removed *in vacuo*, and the residues were dissolved in water and neutralized by NaOH to give sodium 3HHx (3HHx-Na) solution.

Polymer production and analysis

E. coli JM109 was used as the host for plasmid construction and polymer production. *E. coli* was cultivated in 1.5 mL Luria Bertani medium (10 g L^{-1} NaCl, 5 g L^{-1} yeast extract, and 10 g L^{-1} tryptone) containing ampicillin (100 mg L^{-1}) at 30°C for 12 h as the seed culture. For polymer production, cells harboring the plasmid for polymer production were cultivated at 30°C for 48 h. As monomer precursors, 3HB-Na, GL-Na, and 3HHx-Na were added at 1.25 or 2.5 g L^{-1}, 2.5 or 5.0 g L^{-1}, and 0-2.5 g L^{-1}, respectively. The polymer content and monomer composition were analyzed by gas chromatography as described previously (Taguchi *et al.* 2008). The polymer used for subsequent analysis was extracted from cells at 12 or 24 h cultivation. The intracellular polymer in lyophilized cells was extracted using chloroform at 60°C for 48 h.

^{1}H NMR and ^{13}C NMR analyses of the extracted polymer in $CDCl_3$ were carried out as described previously (Arai 2020). The molecular weight of the polymer was measured by size exclusion chromatography using polystyrene standards for calibration, as described previously (Arai 2020).

Preparation of solvent-cast films and mechanical properties analysis

Solvent-cast films of the purified polymers were prepared as follows: Approximately 400 mg of purified polymer was dissolved in 10 mL of chloroform. The

solution was then placed in a glass Petri dish, which was covered with aluminum foil with 10 holes ($\phi \sim 1$ mm), and placed on a horizontal table at room temperature to allow the solution to evaporate. After 2 weeks, the obtained circular film was further dried *in vacuo* for 24 h to remove any residual solvent. The resulting films were stored at room temperature for at least 2 more weeks prior to testing.

The tensile strength, Young's modulus, and elongation to break of the films were determined using a tensile testing machine (EZ-test, Shimadzu, Japan) operated at a tensile speed of 3 mm/min at room temperature. Samples were cut from the films using a dumbbell-shaped cutter SDMP-1000-D (Dumbbell, Japan), with a gauge length and width of 12 mm and 2 mm, respectively.

Thermal properties analysis

The glass transition temperature (T_g) and melting temperature (T_m) of the synthesized polymers were analyzed by differential scanning calorimetry (DSC) analysis using DSC-8500 (PerkinElmer). Approximately 5-10 mg of each polymer was confined in an aluminum pan using a pressing machine (Mettler Toledo). Measurement was performed under nitrogen atmosphere (flow rate: 100 ml/min) at the following temperature control: (1) cooling from 30°C to -30°C at 50°C/min, (2) cooling from -30°C to -50°C at 20°C/min, (3) heating from -50°C to 210°C at 20°C/min, (4) cooling from 210°C to -30°C at 50°C/min, (5) cooling from -30°C to -50°C at 20°C/min, (6) isothermal heating at -50°C for 5 min, and (7) heating from -50°C to 210°C at 20°C/min.

Results and Discussion

Biosynthesis of GL-based PHAs containing 3HHx units

The metabolic pathway used to synthesize PHAs containing GL, 3HB, and

3HHx is shown in Fig. 1. GL, 3HB, and 3HHx were supplemented to the medium and taken up by *E. coli* cells. Propionyl-CoA transferase (PCT) derived from *Megasphaera elsdenii* converts GL and 3HB to GL-CoA and 3HB-CoA, respectively, using acetyl-CoA as a CoA donor. Acyl-CoA ligase (AlkK) activates 3HHx using ATP and free CoA to produce 3HHx-CoA (Wang 2012).

First, we carried out polymer production with various concentrations of 3HHx-Na and fixed concentrations of GL-Na and 3HB-Na (Table 1). In this way, we successfully incorporated 3HHx into the copolymers. The supplemented 3HHx-Na was increased to 2 g L^{-1}, resulting in a subsequent increase in the 3HHx content but a decrease in the relative ratio of GL content within the copolymer (Table 1, No. **1**-**4**). The 3HB fraction incorporated into the copolymers remained nearly constant despite the changing ratios of the other feedstocks. On the other hand, the cell dry weight (CDW) decreased as the 3HHx-Na concentration increased, particularly at concentrations above 2 g L^{-1}, suggesting that 3HHx inhibits cell growth (No. **5**). In contrast, no significant changes in PHA production were observed. When we attempted polymer production in the absence of AlkK, the incorporation of 3HHx decreased compared to that in the presence of AlkK (Table S1). This result clearly demonstrates that AlkK plays an important role in providing 3HHx-CoA for polymer production.

Sequence analysis of 3HHx units

Due to the sequence-regulating capacity of $PhaC_{AR}$, the monomer sequence of the obtained polymer was of interest. Thus, the monomer sequence was analyzed based on changes in NMR chemical shifts influenced by the chemical structures of the adjacent units. The linkages between the 3HB and 3HHx units were determined by the ^{13}C NMR resonances of carbonyl carbons. As shown in Fig. 2 and Fig. S1, three signals, which are ascribed to the carbonyl group of 3HB and 3HHx, were observed at δ 169.0-170.0. These

three signals correspond to the dyad sequences of 3HHx*-3HHx, 3HB*-3HHx or 3HHx*-3HB, and 3HB*-3HB, respectively (Phithakrotchanakoon *et al.* 2015; Shimamura *et al.* 1994). Here, the asterisk indicates the focused unit of which the signal was observed. The abundant 3HB-3HHx/3HHx-3HB linkages indicate that 3HHx units were randomly incorporated into the polymer chain.

The resonances of the carbonyl carbon of the GL units were observed as split peaks in the range of δ 165.0-167.0 due to the triad sequence including GL units (Matsumoto 2011; Matsumoto 2017). However, for the spectrum for polymer **2** which contains 17 mol% GL, the resonance of GL units was not clearly observed due to the low signal intensity. In addition, as GL has a short main-chain, its resonance can be subject to be influenced by the adjacent monomer units. The signal of the carbonyl carbon of GL is predicted to be divided into nine triad patterns (3HB/3HHx/GL-GL*-3HB/3HHx/GL), therefore the intensity could be very weak to be detected. Indeed, for another terpolymer harboring 19 mol% GL, the signals were slightly observed (Fig. S2).

Sequence analysis of GL units

Previous research has demonstrated that the ^{1}H NMR resonance of the methylene proton of GL in P(GL-*ran*-3HB) is observed as four characteristic signals at 4.5-4.9 ppm, which are ascribed to GL-GL*-GL (a), GL-GL*-3HB or 3HB-GL*-GL [(b) or (c)], and 3HB-GL*-3HB (d) triad sequences, respectively (Fig. 3) (Arai 2020; Matsumoto 2017). Similarly, the terpolymer exhibits four similar signals that correspond to GL-GL*-GL (a), GL-GL*-(3HB/3HHx) or (3HB/3HHx)-GL*-GL [(b) or (c)], and (3HB/3HHx)-GL*-(3HB/3HHx) (d), respectively (Fig. S3). The effects of 3HB and 3HHx units in the triads on the chemical shift of the GL proton were indistinguishable. Based on the relative intensities of the four signals, the local GL fraction, which is defined as the molar ratio of GL units in a segment of P(GL-*co*-3HB) (Arai 2020), can be calculated (Table 1, Table

S2). In our previous study, for example, we found that P(40 mol% GL-*co*-3HB) has a GL-rich segment in which the local GL fraction is estimated to be 71 mol% (Arai 2020). Here, we calculated the local GL fraction of the terpolymer in the same way (Table 1, Table S2). In all of the polymers produced and analyzed, the local GL fractions were higher than the total GL fractions, clearly indicating the heterologous distribution of GL units in the polymer chain. For polymer **1** P(GL-*co*-3HB), the resonance pattern was similar to that in our previous study (Arai 2020). The intensity of (a) (***a*** in Table S2**)** was the highest among the four signals, followed by ***b*** and ***c***, and ***d*** was the lowest (Table S2). This result demonstrates that the GL-rich segment is present in polymer **1**. For polymers **2**-**4**, as the 3HHx fraction increased, ***a***-***c*** decreased whereas ***d*** increased. The local GL fraction of polymer **2** was 56 mol% (Table 1). The ratio of the GL-rich segment in **1** was estimated to be 39%, which is higher than that in **2** and **3** (30%), whereas the ratio and the local GL fraction of **4** could not be determined due to its low signal intensity of GL units. Therefore, the ratio of the GL-rich segment was reduced by the incorporation of 3HHx.

Based on the results of NMR analysis, we propose the polymer structures (Fig. 4). The structure for polymer **1** is similar to that observed in our previous study, which is P(GL-*ran*-3HB)-*b*-P(3HB) (Arai 2020). For polymer **2**, the ^{13}C NMR results suggest the presence of a P(3HB-*co*-3HHx) segment while ^{1}H NMR suggests the presence of a terpolymer segment. Thus, **2** can be presumed to be P(3HB-*co*-3HHx)-*b*-P(GL-*co*-3HB-*co*-3HHx). The monomer sequence in each segment is presumably random, although the statistical randomness in the terpolymer segment cannot be determined from the obtained data. For polymer **4**, the GL-rich segment disappeared; thus, it is presumed to be P(GL-*co*-3HB-*co*-3HHx).

It should be noted that the current analysis does not determine the number and the order of the segments. Fig. 4 depicted the total amount (ratio) of each segment, but does not necessarily mean that the obtain polymer is a diblock copolymer.

231

232 **Mechanical properties of solvent-cast films**

233 The solvent-cast film of P(20 mol% GL-*co*-3HB) (Arai 2020) was opaque due
234 to the high crystallinity of P(3HB), whereas those of polymers **2** and **3** were transparent
235 (Fig. 5). These results suggest that the incorporation of 3HHx lowers the crystallinity of
236 the polymers. Next, stress-strain tests were carried out on the films at room temperature
237 (Fig. S4 and Table 2). The Young's modulus of polymers **2** and **3** [P(GL-*co*-3HB-*co*-
238 3HHx)] was much lower than that of **1** [P(GL-*co*-3HB)] and PHBH, indicating that the
239 terpolymer is a very soft and extensible material.

240

241 **Thermal properties of the polymers**

242 The thermal properties of the synthesized polymers were determined (Fig. 6 and
243 Table 3). Polymer **1** exhibited a melting peak at 157.6°C, which can be ascribed to the
244 relatively large crystalline fraction of P(3HB). For the polymers containing 3HHx, as the
245 3HHx fraction increased, the area of the melting peak decreased and eventually
246 disappeared. This result indicates that the incorporation of 3HHx units drastically lowered
247 the crystallinity of the polymer, and that the P(3HB) homopolymer segment does not exist
248 in polymers **2**-**4**. This finding is consistent with appearance and physical properties of the
249 solvent-cast films described above and further supports the proposed structures shown in
250 Fig. 4.

251

252

253 **Conclusions**

254 The sequence-regulating PHA synthase $PhaC_{AR}$ synthesized a novel GL-based
255 terpolymer P(3HB-*co*-3HHx)-*b*-P(GL-*co*-3HB-*co*-3HHx), which is the first PHA block
256 copolymer composed of two random copolymer segments. An inverse relationship was

observed between GL and 3HHx fractions. In addition, the ratio of GL-containing segments was reduced by introducing 3HHx units. However, the mechanism of this phenomenon at the molecular level remains unclear. To achieve the combination of hydrolytic degradability and flexible properties, a greater ratio of GL-rich segments containing 3HHx units is preferable. Therefore, further improvement of the biosynthetic system is needed. The hydrolytic degradability and bioabsorption of the terpolymer and P(GL-*co*-3HB) synthesized using PhaC1$_{Ps}$STQK will be addressed in our future work.

Authors' contributions

H.T. analyzed data and wrote the manuscript. K.S. performed the experiments, analyzed data, and wrote the manuscript. C.N. provided the *alkK* gene and wrote the manuscript. K.M. designed and supervised this study, analyzed data, and wrote the manuscript. All authors read and approved the final version of the manuscript.

Acknowledgments and Funding

This work was supported by the JST-Mirai Program (No. JPMJMI19EB) and JSPS Kakenhi (20H04368).

Conflict of Interest

The authors declare no conflict of interest.

Data Availability Statement

The data underlying this article are available in the article and in its online supplementary material.

References

Arai S, Sakakibara S, Mareschal R et al. Biosynthesis of random-homo block copolymer poly[glycolate-*ran*-3-hydroxybutyrate (3HB)]-*b*-Poly(3HB) using sequence-regulating chimeric polyhydroxyalkanoate synthase in *Escherichia coli*. *Front Bioeng Biotechnol* 2020;8:612991.

Bedade DK, Edson CB, and Gross RA. Emergent approaches to efficient and sustainable polyhydroxyalkanoate production. *Molecules* 2021;26:3463.

Bartels M, Gutschmann B, Widmer T et al. Recovery of the PHA copolymer P(HB-*co*-HHx) with non-halogenated solvents: influences on molecular weight and HHx-content. *Front Bioeng Biotechnol* 2020;8:944.

Basnett P, Marcello E, Lukasiewicz B et al. Biosynthesis and characterization of a novel, biocompatible medium chain length polyhydroxyalkanoate by *Pseudomonas mendocina* CH50 using coconut oil as the carbon source. *J Mater Sci Mater Med* 2018;29:179.

Chen GQ, Zhang J. Microbial polyhydroxyalkanoates as medical implant biomaterials. *Artif Cells Nanomed Biotechnol* 2018;46:1-18.

Doi Y, Kitamura S, and Abe H. Microbial synthesis and characterization of poly(3-hydroxybutyrate-*co*-3-hydroxyhexanoate). *Macromolecules* 1995;28:4822-4828.

Matsumoto K, Hori C, Fujii R et al. Dynamic changes of intracellular monomer levels regulate block sequence of polyhydroxyalkanoates in engineered *Escherichia coli*.

Biomacromolecules 2018;19:662-71.

Matsumoto K, Ishiyama A, Sakai K et al. Biosynthesis of glycolate-based polyesters containing medium-chain-length 3-hydroxyalkanoates in recombinant *Escherichia coli* expressing engineered polyhydroxyalkanoate synthase. *J Biotechnol* 2011;156:214-7.

Matsumoto K, Shiba T, Hiraide Y et al. Incorporation of glycolate units promotes hydrolytic degradation in flexible poly(glycolate-*co*-3-hydroxybutyrate) synthesized by engineered *Escherichia coli*. *ACS Biomater Sci Eng* 2017;3:3058-63.

Matsumoto K, Takase K, Yamamoto Y et al. Chimeric enzyme composed of polyhydroxyalkanoate (PHA) synthases from *Ralstonia eutropha* and *Aeromonas caviae* enhances production of PHAs in recombinant *Escherichia coli*. *Biomacromolecules* 2009;10:682-5.

Pandita D, Kumar S, Lather V. Hybrid poly(lactic-*co*-glycolic acid) nanoparticles: design and delivery prospectives. *Drug Discov Today* 2015;20:95-104.

Pervaiz F, Ahmad M, Li L et al. Development and characterization of olanzapine loaded poly(lactide-*co*-glycolide) microspheres for depot injection: *in vitro* and *in vivo* release profiles. *Curr Drug Deliv* 2019;16:375-83.

Phithakrotchanakoon C, Champreda V, Aiba S-I et al. Production of polyhydroxyalkanoates from crude glycerol using recombinant *Escherichia coli*. *J Polym Environ* 2015;23:38-44.

Rehm BH. Polyester synthases: natural catalysts for plastics. *Biochem J* 2003;376:15-33.

Rehm BH, Krüger N, Steinbüchel A. A new metabolic link between fatty acid *de novo* synthesis and polyhydroxyalkanoic acid synthesis. The PHAG gene from *Pseudomonas putida* KT2440 encodes a 3-hydroxyacyl-acyl carrier protein-coenzyme a transferase. *J Biol Chem* 1998;273:24044-51.

Sato S, Maruyama H, Fujiki T et al. Regulation of 3-hydroxyhexanoate composition in PHBH synthesized by recombinant *Cupriavidus necator* H16 from plant oil by using butyrate as a co-substrate. *J Biosci Bioeng* 2015;120:246-51.

Satoh Y, Murakami F, Tajima K et al. Enzymatic synthesis of poly(3-hydroxybutyrate-*co*-4-hydroxybutyrate) with CoA recycling using polyhydroxyalkanoate synthase and acyl-CoA synthetase. *J Biosci Bioeng* 2005;99:508-11.

Scheel RA, Fusi AD, Min BC et al. Increased production of the value-added biopolymers poly(*R*-3-hydroxyalkanoate) and Poly(γ-glutamic acid) from hydrolyzed paper recycling waste fines. *Front Bioeng Biotechnol* 2019;7:409.

Shawe S, Buchanan F, Harkin-Jones E et al. A study on the rate of degradation of the bioabsorbable polymer polyglycolic acid (PGA). *J Mater Sci* 2006;41:4832-38.

Shimamura E, Kasuya K, Kobayashi G et al. Physical properties and biodegradability of microbial poly(3-hydroxybutyrate-*co*-3-hydroxyhexanoate). *Macromolecules* 1994;27:878-80.

361 Steinbüchel A and Hein S. Biochemical and molecular basis of microbial synthesis of
362 polyhydroxyalkanoates in microorganisms. *Adv Biochem Eng Biotechnol* 2001;71:81-
363 123.
364
365 Sudesh K, Abe H, and Doi Y. Synthesis, structure and properties of
366 polyhydroxyalkanoates: biological polymers. *Prog Polym Sci* 2000;25:1503-1555.
367
368 Taguchi S, Yamada M, Matsumoto K et al. A microbial factory for lactate-based
369 polyesters using a lactate-polymerizing enzyme. *Proc Natl Acad Sci USA*
370 2008;105:17323-7.
371
372 Tappel RC, Pan W, Bergey NS et al. Engineering *Escherichia coli* for improved
373 production of short-chain-length-*co*-medium-chain-length poly[(*R*)-3-hydroxyalkanoate]
374 (SCL-*co*-MCL PHA) copolymers from renewable nonfatty acid feedstocks. *ACS Sustain*
375 *Chem Eng* 2014;2;1879-1887.
376
377 Wang Q, Tappel RC, Zhu C et al. Development of a new strategy for production of
378 medium-chain-length polyhydroxyalkanoates by recombinant *Escherichia coli* via
379 inexpensive non-fatty acid feedstocks. *Appl Environ Microbiol* 2012;78:519-27.
380
381 Wong YM, Brigham CJ, Rha C et al. Biosynthesis and characterization of
382 polyhydroxyalkanoate containing high 3-hydroxyhexanoate monomer fraction from
383 crude palm kernel oil by recombinant *Cupriavidus necator*. *Bioresour Technol*
384 2012;121:320-7.
385
386 Zhang J, Shishatskaya EI, Volova TG et al. Polyhydroxyalkanoates (PHA) for therapeutic

applications. *Mater Sci Eng C Mater Biol Appl* 2018;86:144-50.

391 **Tables**

392

393 Table 1. Synthesis of the GL-based polymers containing 3HHx.

No.	Precursor Conc.*[1] (g L^{-1})			CDW (g L^{-1})	Polymer production (g L^{-1})	Monomer composition (mol%)			Local GL fraction (mol%)	Molecular weight		
	GL	3HB	3HHx			GL	3HB	3HHx		M_n (× 10^4)	M_w (× 10^4)	M_w/M_n
1	2.50	2.50	0.00	3.75 ± 0.11	0.37 ± 0.03	27	73	0	68	2.6	5.4	2.1
2			0.50	3.28 ± 0.23	0.37 ± 0.07	17	68	15	56	6.9	9.9	1.4
3			1.00	3.15 ± 0.20	0.45 ± 0.07	9	64	27	30	6.5	15	2.3
4			1.50	2.45 ± 1.22	0.37 ± 0.14	5	59	36	-*[2]	13	21	1.6

394 *[1]Concentrations of precursors are shown as sodium salts. *[2]The local GL fraction of **4**
395 could not be calculated due to the low signal intensity. CDW: cell dry weight, M_w:
396 weight average molecular weight, M_n: number average molecular weight. -: Not tested
397 due to poor cell growth. Values are the average ± standard deviation of data from three
398 independent experiments.
399

400 Table 2. Mechanical properties of GL-based PHAs.

No.	Film composition	Tensile strength (MPa)	Young's modulus (MPa)	Elongation to break (%)
-*	P(20 mol% GL-*co*-3HB)	16	348	7
2	P(17 mol% GL-*co*-3HB-*co*-15 mol% 3HHx)	1.3	63	8
3	P(9 mol% GL-*co*-3HB-*co*-27 mol% 3HHx)	1.0	7.2	43

401 *This polymer was synthesized and reported in our previous study (Arai 2020).

402

403

404 Table 3. Thermal properties of the synthesized polymers.

Polymer	Monomer composition (mol%)			T_g (°C)	T_m (°C)	ΔH (J g^{-1})
	GL	3HB	3HHx			
1	27	73	0	-0.6	157.6	43.5
2	17	68	15	-2.5	118.9	21.3
3	9	64	27	-5.2	116.9	2.3
4	5	59	36	-10.5	ND	ND

405 ND, Not detected.

406

407

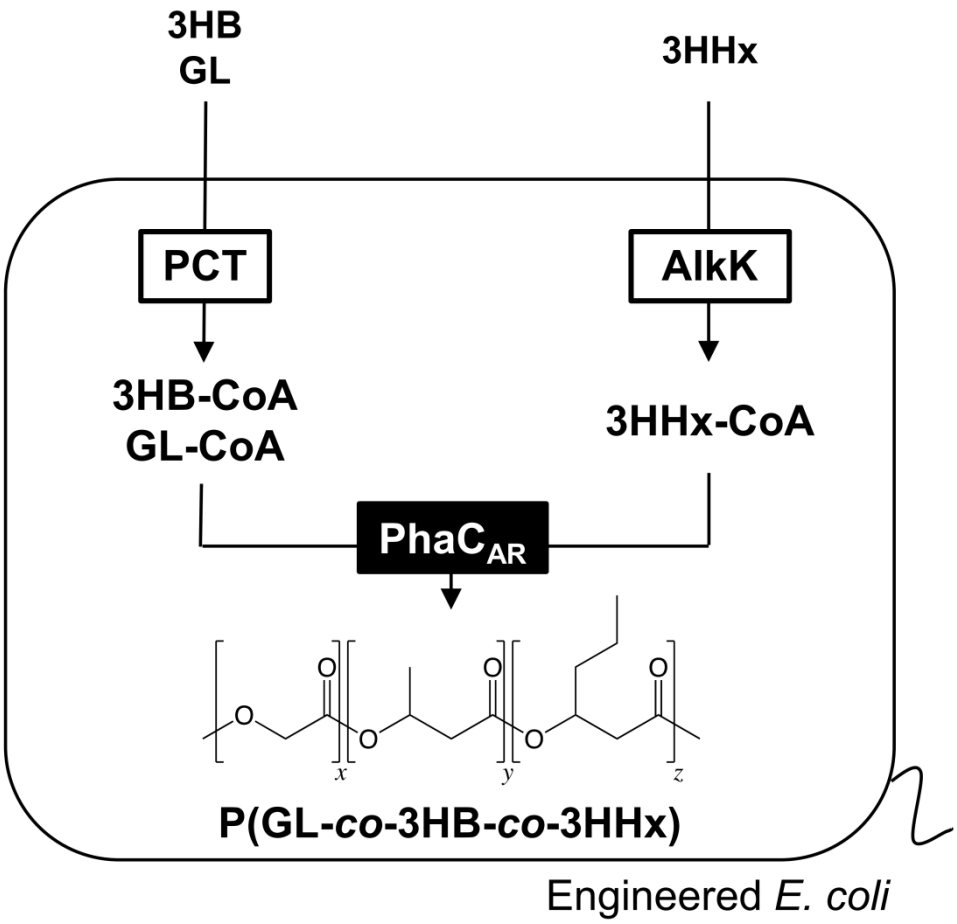

Figure 1. Illustration of the metabolic pathway used in this study to synthesize the terpolymer P(GL-*co*-3HB-*co*-3HHx) in *E. coli*. Propionyl-CoA transferase (PCT) transfers CoA from acetyl-CoA to GL and 3HB, thereby producing GL-CoA and 3HB-CoA. Acyl-CoA ligase (AlkK) is an ATP-dependent enzyme that activates 3HHx into 3HHx-CoA . $PhaC_{AR}$ polymerizes the CoA thioesters.

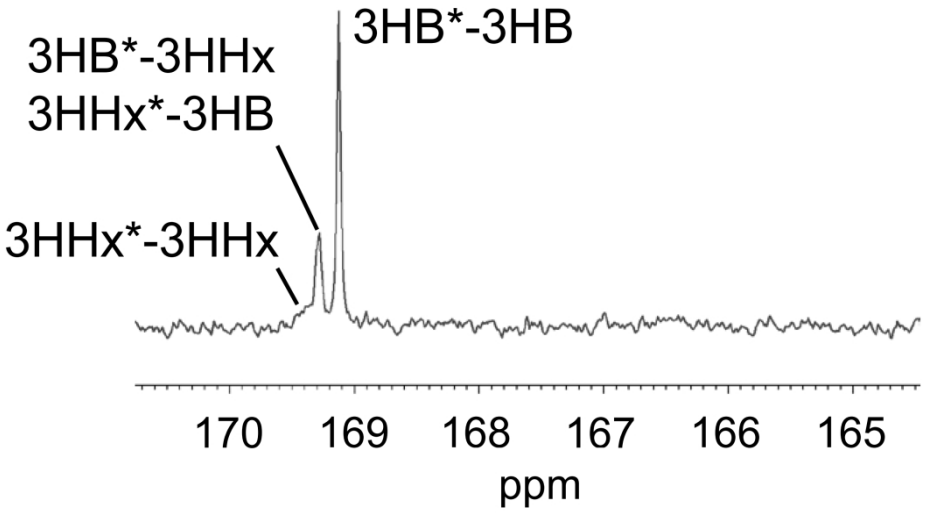

Figure 2. ^{13}C NMR spectrum of polymer **2**. Peaks correspond to the indicated dyads. GL-containing dyad peaks appear at δ 165-167. The overall spectrum is shown in Fig. S1.

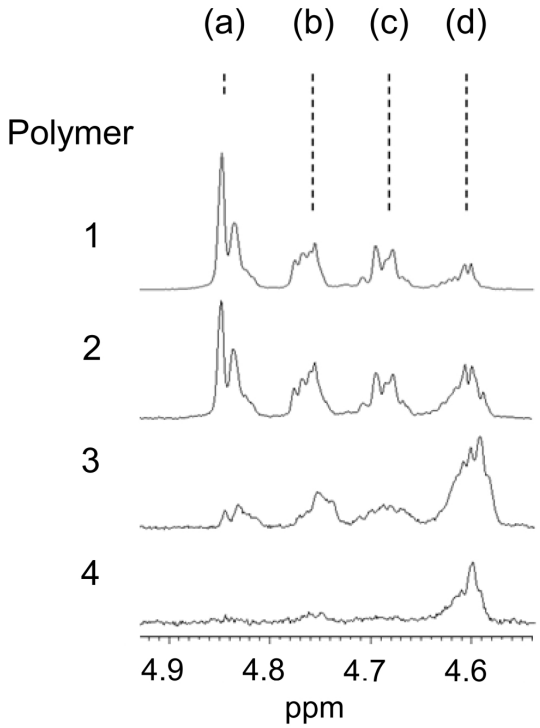

Figure 3. Partial ^{1}H NMR spectra of polymers **1**-**4**. Peaks (a)-(d) correspond to the monomer triads: GL-GL*-GL (a), GL-GL*-(3HB/3HHx) and (3HB/3HHx)-GL*-GL ((b) or (c)), and (3HB/3HHx)-GL*-(3HB/3HHx) (d), respectively. The full spectra are shown in Fig. S3.

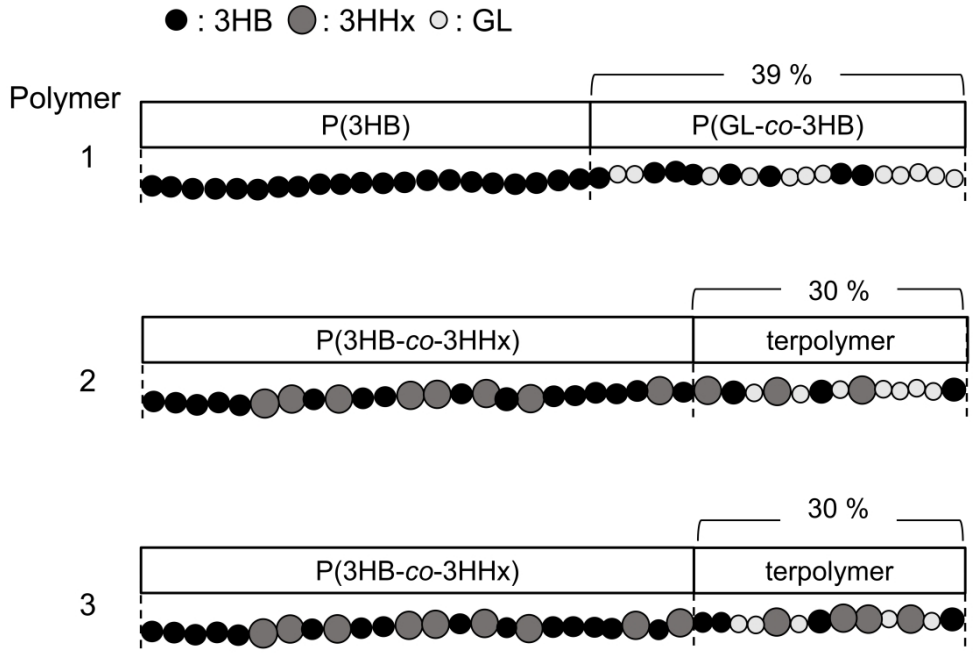

Figure 4. Proposed sequence structures of P(GL-*co*-3HB-*co*-3HHx) synthesized using PhaC$_{AR}$. The number and the order of the segments are not determined.

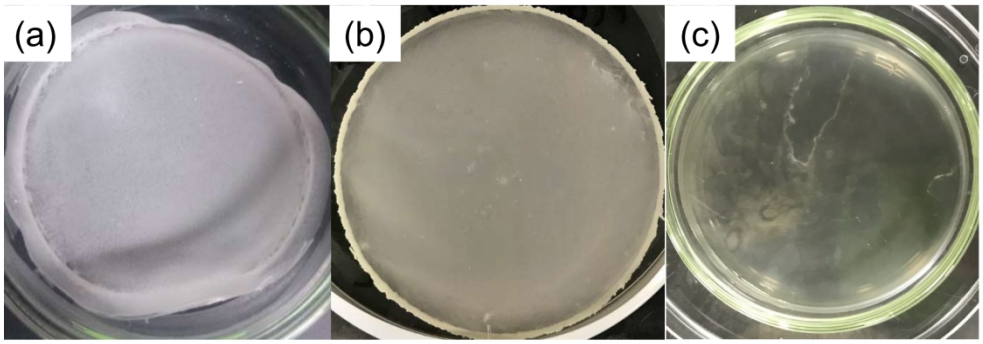

Figure 5. The appearance of the solvent-cast films. (a) P(20 mol% GL-*co*-3HB) (Arai 2020), (b) P(17 mol% GL-*co*-3HB-*co*-15 mol% 3HHx) (**2**), and (c) P(9 mol% GL-*co*-3HB-*co*-27 mol% 3HHx) (**3**).

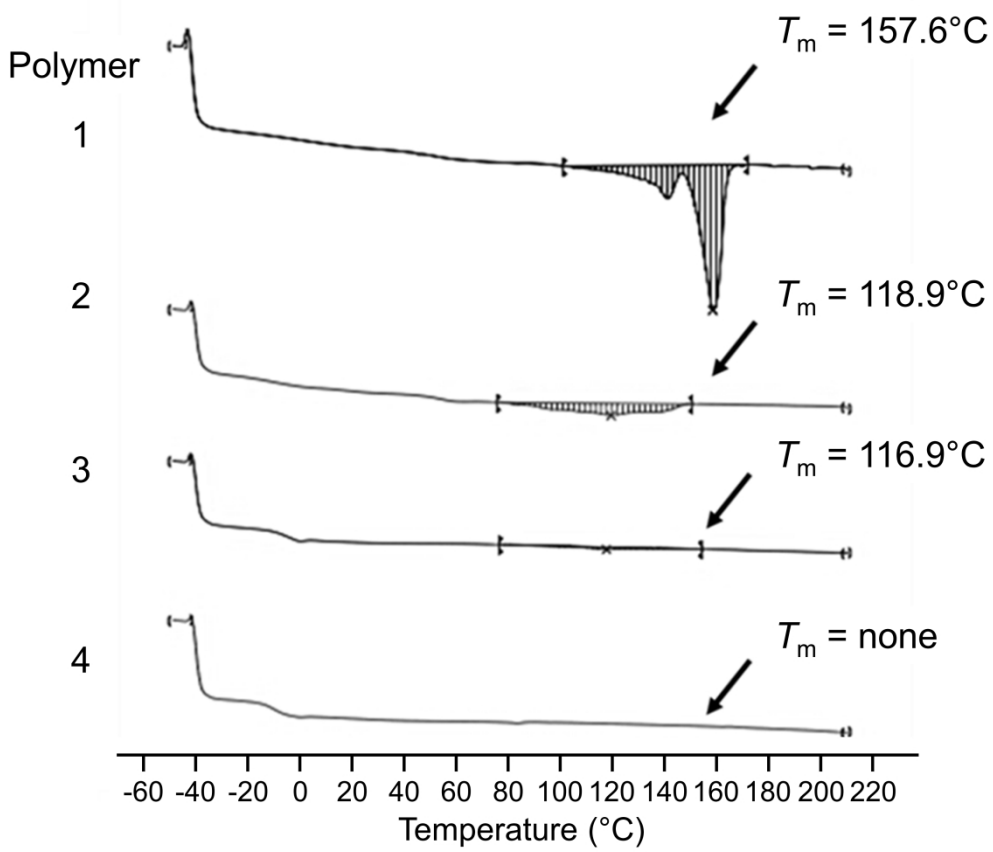

435

436 Figure. 6. DSC analysis of the synthesized polymers.

437

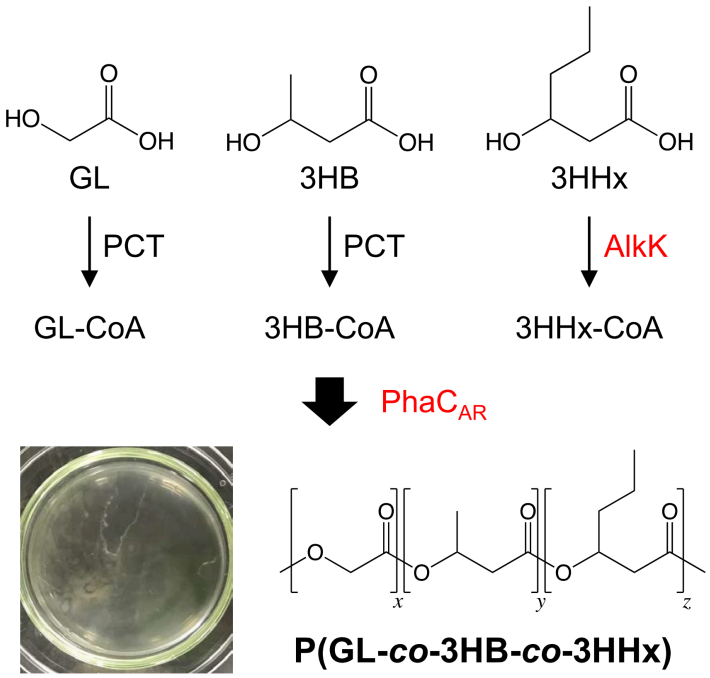

438

439 Graphical Abstract Caption

440 A novel terpolymer P(GL-*co*-3HB-*co*-3HHx) was produced using PCT and AlkK for

441 monomer supply and PhaC$_{AR}$ for polymerization in *Escherichia coli*.

442 **Supplementary materials**

443

444 Table S1. The effects of *alkK* on the incorporation of 3HHx into the polymer.

Plasmid	Precursor Conc.* (g L^{-1})			CDW (g L^{-1})	Polymer production (g L^{-1})	Monomer composition (mol%)		
	GL	3HB	3HHx			GL	3HB	3HHx
pBSPRephaC$_{AR}$pct	2.5	2.5	0.0	3.19 ± 0.02	0.26 ± 0.01	25	75	0
			1.0	2.79 ± 0.12	0.36 ± 0.00	19	81	0
pBSPRephaC$_{AR}$pctAlkK	2.5	2.5	0.0	3.49 ± 0.05	0.42 ± 0.02	23	77	0
			1.0	3.30 ± 0.19	0.47 ± 0.01	9	65	26

445 *Concentrations of precursors are shown as sodium salts. CDW: cell dry weight. Values

446 are the average ± standard deviation of data from three independent experiments.

447

448

Table S2. Monomer sequence analysis based on ^{1}H NMR.

	GL ratio (mol%)	3HB and 3HHx ratio (mol%)	Relative intensity of GL units in the triad sequences (%)*1				Local GL fraction*2
			a	***b***	***c***	***d***	
Synthesized polymer **1**	27	73	46.6 ± 3.0	21.0 ± 0.2	22.7 ± 2.0	9.8 ± 1.3	68
Calculated ideal random polymer	68	32	46	22	22	10	
Synthesized polymer **2**	17	83	33.9 ± 9.0	21.7 ± 0.7	22.2 ± 2.8	22.3 ± 6.4	56
Calculated ideal random polymer	56	44	31	25	25	19	
Synthesized polymer **3**	9	91	13.2 ± 1.6	21.4 ± 0.9	16.0 ± 1.9	49.3 ± 1.6	30
Calculated ideal random polymer	30	70	9	21	21	49	

*1 For the synthesized polymers, the values ***a*-*d*** were calculated as previously described (Arai 2020). Briefly, using the function *Area*, which is the ^{1}H NMR peak area of the molecular species, ***a*** is defined as Area(a)/[Area (a) + Area(b) + Area(c) + Area(d)]; ***b***, ***c***, and ***d*** are defined in the same manner. For the ideal polymers, ***a*** was calculated as x^2, where x is the GL ratio (mol%); ***b*** and ***c***, and ***d*** were calculated as $x(1\text{-}x)$ and $(1\text{-}x)^2$, respectively. *2 The local GL fraction (x mol%) for the calculated ideal random polymers was calculated as the residual sum of squares of the measured values of ***a*-*d*** for the synthesized polymers and the calculated values of ***a*-*d*** for the ideal polymers. Using the function $\Delta(y)$, which is defined as [***y***(measured) – ***y***(calculated)] (where $y = a, b, c, d$), the GL ratio x is defined as the value that gives the minimum of $\Sigma(y = a, b, c, d)\ [\Delta(y)]^2$. The ratio of the P(3HB-*co*-3HHx) segment [P(3HB-*co*-3HHx)] was calculated using the equation: [P(3HB-*co*-3HHx)] = [total 3HB + 3HHx] – [total GL] x $(1\text{-}x)/x$.

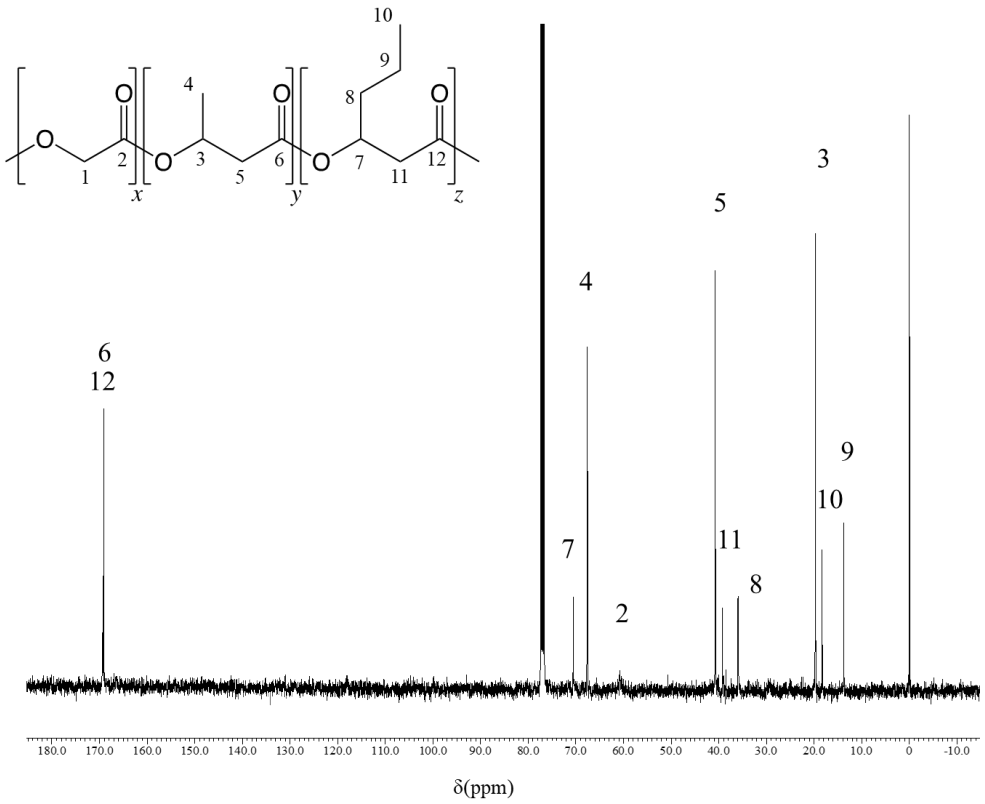

463

464 Figure S1. ^{13}C NMR of polymer **2**.

465

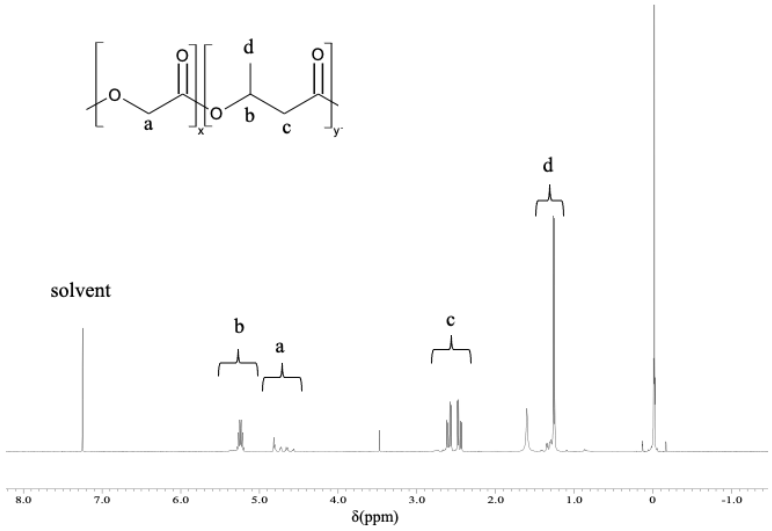

466

467 Figure S2a. ^{1}H NMR of polymer **1**.

468

469 Figure S2b. ^{1}H NMR of polymer **2**.

470

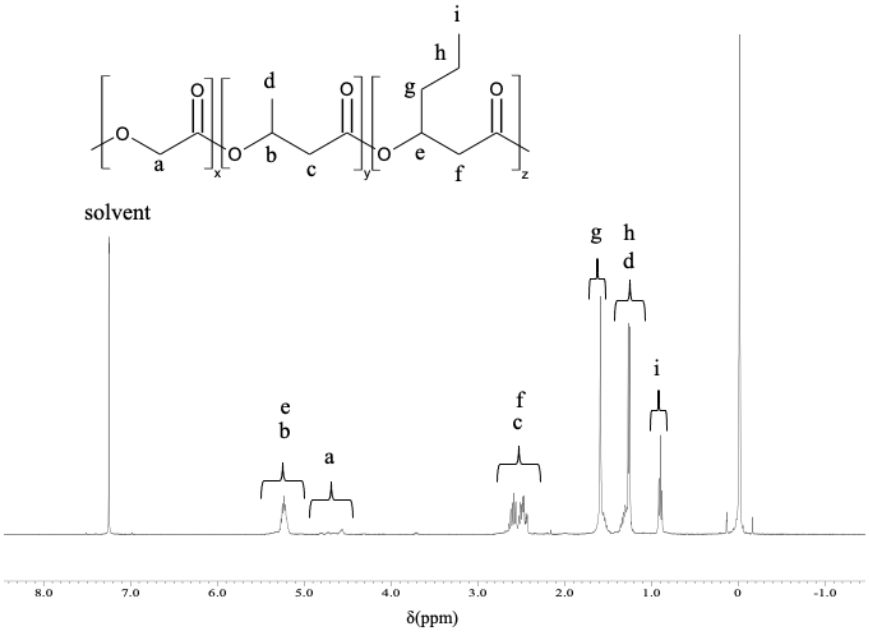

471

472 Figure S2c. ^{1}H NMR of polymer **3**.

473

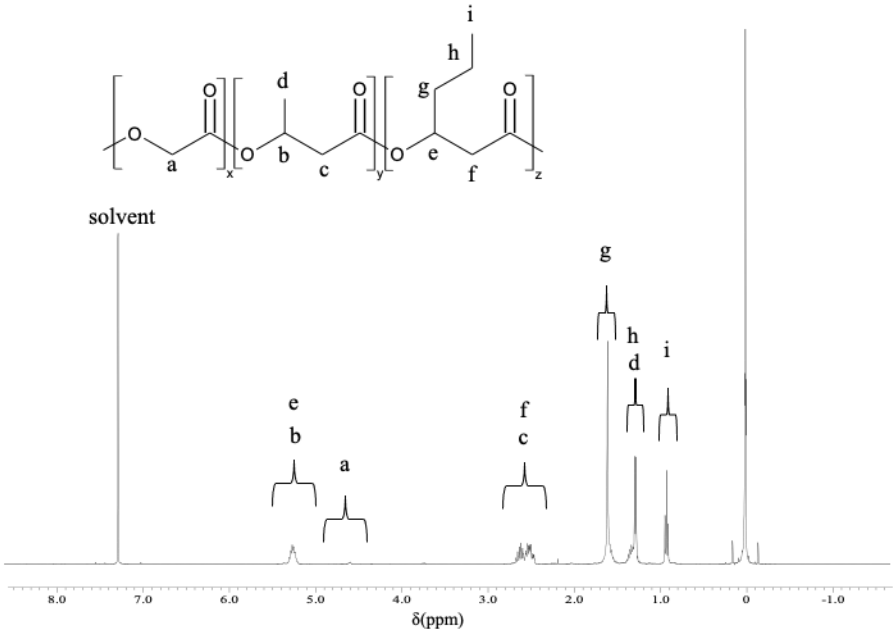

474

475 Figure S2d. ^{1}H NMR of polymer **4**.

476

477

478

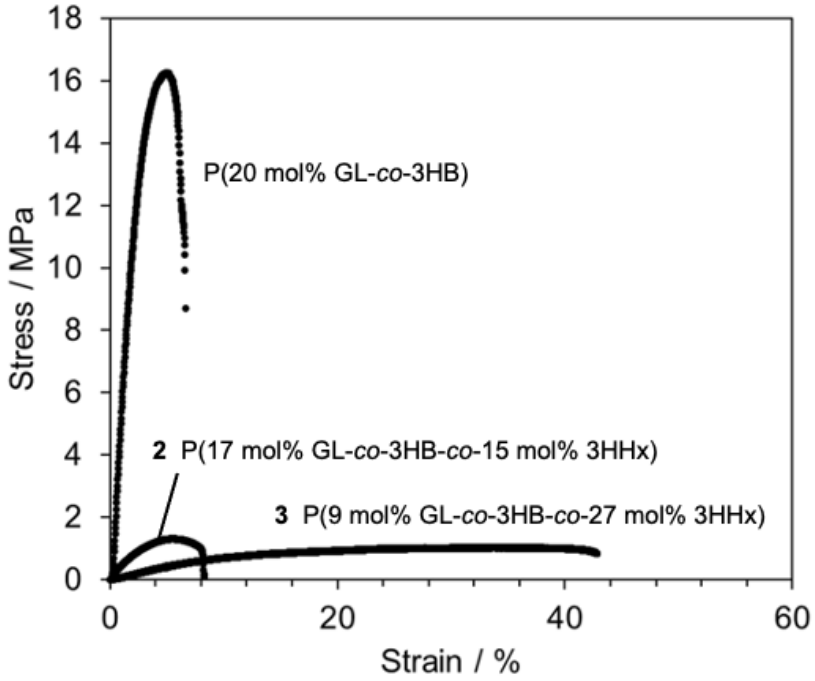

Figure S3. Stress-strain curve.